



# Determining whether the diagnostic value of B-ultrasound combined with contrast-enhanced ultrasound and shear wave elastography in breast mass-like and non-mass-like lesions differs: a diagnostic test

Shi-Yu Li<sup>1</sup>, Rui-Lan Niu<sup>1</sup>, Bo Wang<sup>1</sup>, Ying Jiang<sup>1</sup>, Jia-Nan Li, Gang Liu<sup>2</sup>, Zhi-Li Wang<sup>1</sup>

<sup>1</sup>Department of Ultrasound, The First Medical Center of PLA General Hospital, Beijing, China; <sup>2</sup>Department of Radiology, The First Medical Center of PLA General Hospital, Beijing, China

**Contributions:** (I) Conception and design: G Liu, ZL Wang; (II) Administrative support: G Liu, ZL Wang; (III) Provision of study materials or patients: SY Li, RL Niu; (IV) Collection and assembly of data: B Wang, Y Jiang; (V) Data analysis and interpretation: SY Li, JN Li; (VI) Manuscript writing: All authors; (VII) Final approval of manuscript: All authors.

**Correspondence to:** Zhi-Li Wang. Department of Ultrasound, The First Medical Center of PLA General Hospital, 28 Fuxing Road, Beijing 100853, China. Email: wzllg@sina.com; Gang Liu. Department of Radiology, The First Medical Center of PLA General Hospital, 28 Fuxing Road, Beijing 100853, China. Email: lgwzl@126.com.

**Background:** Mass-like (ML) and non-mass-like (NML) are two manifestations of breast lesions on ultrasound. Contrast-enhanced ultrasound (CEUS) can make up for the limitation of B-ultrasound (US) in the observation of focal blood flow, and shear wave elastography (SWE) can supplement the hardness information of the lesion. The present study aimed to analyze the characteristic manifestations of US, CEUS, and SWE in NML and ML breast and evaluate whether the diagnostic performance of these three ultrasound techniques differs in terms of differentiating between benign and malignant breast lesions.

**Methods:** From January to August 2021, 382 patients (417 breast lesions) underwent US, CEUS, and SWE examinations. Of these, 204 women (218 breast lesions) were included in our study due to subsequent biopsy or surgery with pathological findings. The patients were divided into ML and NML groups according to the ultrasound characteristics, and the differences in multimodal ultrasound performance between benign and malignant NML and benign and malignant ML breast lesions were compared. The diagnostic performance of US, US + CEUS, US + SWE, US + CEUS + SWE for ML, NML and all breast lesions was evaluated by analyzing sensitivity, specificity and area under receiver operating characteristic (ROC) curve (AUC).

**Results:** Pathologically, the 218 lesions included 96 malignant and 122 benign breast lesions. The sensitivity and specificity of US + CEUS + SWE in all lesion groups, ML group and NML group were 92.7% and 90.2%, 95.9% and 90.3%, 91.3% and 79.3%, respectively. In all breast group, AUCs of US + CEUS, US + SWE, US + CEUS + SWE were statistically different from AUC of US ( $P=0.0010$ ,  $0.0001$ ,  $0.0001$ ). In the ML group, the AUC of US + CEUS, US + SWE, US + CEUS + SWE were statistically different from that of US ( $P=0.0120$ ,  $0.0008$ ,  $0.0002$ ). In the NML group, there was a statistical difference between US + SWE and US AUC ( $P=0.0149$ ).

**Conclusions:** US, CEUS, and SWE have an important diagnostic value for benign and malignant ML and NML breast lesions. Multimodal ultrasound combined with US, CEUS, and SWE can improve the diagnostic efficacy in distinguishing between benign and malignant ML and NML lesions.

**Keywords:** B-ultrasound; contrast-enhanced ultrasound (CEUS); shear wave elastography (SWE); mass-like breast lesion (ML); non-mass-like breast lesion (NML)

Submitted Jan 31, 2023. Accepted for publication Feb 16, 2023. Published online Feb 24, 2023.

doi: 10.21037/gs-23-51

View this article at: <https://dx.doi.org/10.21037/gs-23-51>

## Introduction

Breast cancer, which exhibits varying manifestations among women, has resulted in global human suffering and premature death burden in many countries over the past few decades (1). Routine screening is a very important conventional means for detecting breast cancer to improve diagnostic levels. Several early diagnostic methods and treatments for breast cancer have reduced the mortality rate and prolonged the survival time of patients (2,3). Ultrasound (US) is a widely used auxiliary method for detecting breast lesions because of its low cost, convenience, and absence of radiation (4). Breast lesions can manifest as mass-like (ML) or non-mass-like (NML) breast lesions on US (5). NML lesions are rarer than ML lesions, accounting for only 9.2% of breast lesions (6). Moreover, since NML lesions do not have obvious boundaries on both sections of conventional US, they are more difficult to identify than ML (7).

At present, the most used breast disease classification system is the breast imaging report and data system (BI-RADS), which is applied to assess the possibility of malignant breast lesions in a more standardized and objective way on US (8). Owing to a certain degree of overlap in the atypical features and morphological characteristics of BI-RADS 3–5 breast diseases, it is not enough to identify benign and malignant lesions by the conventional US alone (9). In recent years, based on traditional US, some relatively new ultrasonic technologies,

such as contrast-enhanced ultrasound (CEUS) and shear wave elastography (SWE), have gradually been developed to make up for the lack to compensate for the limitations of conventional US (10,11). Numerous studies have suggested that with the gradual improvement of CEUS and SWE, their diagnostic accuracy for breast diseases has improved considerably (12,13).

Blood perfusion in breast lesions can be observed by CEUS (14). Blood perfusion in the lesion tends to affect its growth, development, infiltration, and metastasis (15,16). CEUS can display microbubbles in the time dimension, reflecting the blood supply in the scanning area and more accurately representing the size of the lesion (17). The maximum value measured by CEUS is closer to the pathological measurement of surgical specimens (18). Compared with the conventional US, the diagnostic function of CEUS in identifying mammary malignant and benign diseases has been evaluated in massive studies (19,20). Zhou *et al.* demonstrated CEUS possesses excellent overall sensitivity [0.88, 95% confidence interval (CI): 0.86–0.89] and specificity (0.82, 95% CI: 0.80–0.83) for the qualitative analysis of breast lesions (14).

SWE, another new related ultrasonographic technique, utilizes the elastic properties of tissue to assess the stiffness of lesions (11). With its high repeatability, SWE has also been widely applied for diagnosing substantial superficial diseases, especially breast neoplasms (21). Numerous researchers in China and abroad have employed this technique for breast examination and believe that the elasticity coefficients of different tissues in the breast vary (13,22); the greater the elastic coefficient of the organization, the greater its hardness (23). Since Athanasiou *et al.* (24) first reported that malignant lesions are often more dense than benign lesions on SWE, many reports have subsequently verified this finding, probably due to malignant pathological changes being typically accompanied by more collagen and elastin (21,25). Farooq *et al.* demonstrated that SWE had high sensitivity (92.17%), specificity (90.4%), and diagnostic accuracy (91.61%) in distinguishing between benign and malignant breast lesions (26). He *et al.* proved  $E_{mean} + I_{mean}$  and  $E_{max} + E_{mean} + I_{mean}$  of shell at 1.0 mm both had the highest area under the curve (AUC) of 0.86 [95% confidence interval (CI): 0.67, 0.96] and SWE synchronous CEUS could effectively improve the diagnostic ability of breast lesions (27). Also, a study by Liu *et al.* showed that the sensitivity and specificity of US + CEUS + SWE were 97.7% and 93.2%, which could improve the diagnostic reliability of breast US-BI-RADS 3 and 4 lesions (9). Hitherto, the

### Highlight box

#### Key findings

- Multimodal ultrasound combined with B-ultrasound (US), contrast-enhanced ultrasound (CEUS), and shear wave elastography (SWE) can improve the diagnostic efficacy for distinguishing benign and malignant non-mass-like (NML) and mass-like (ML) breast lesions.

#### What is known and what is new?

- The accuracy of conventional ultrasound diagnosis of NML needs to be improved. The application of multimodal ultrasound can improve the diagnostic efficiency for NML.
- This paper compares the diagnostic efficacy of multimodal ultrasound for NML and ML breast lesions.

#### What are the implications, and what should change now?

- In subsequent research, we should expand the sample size and conduct a multi-center study to verify the diagnostic efficacy of multimodal ultrasound for NML and ML breast lesions.

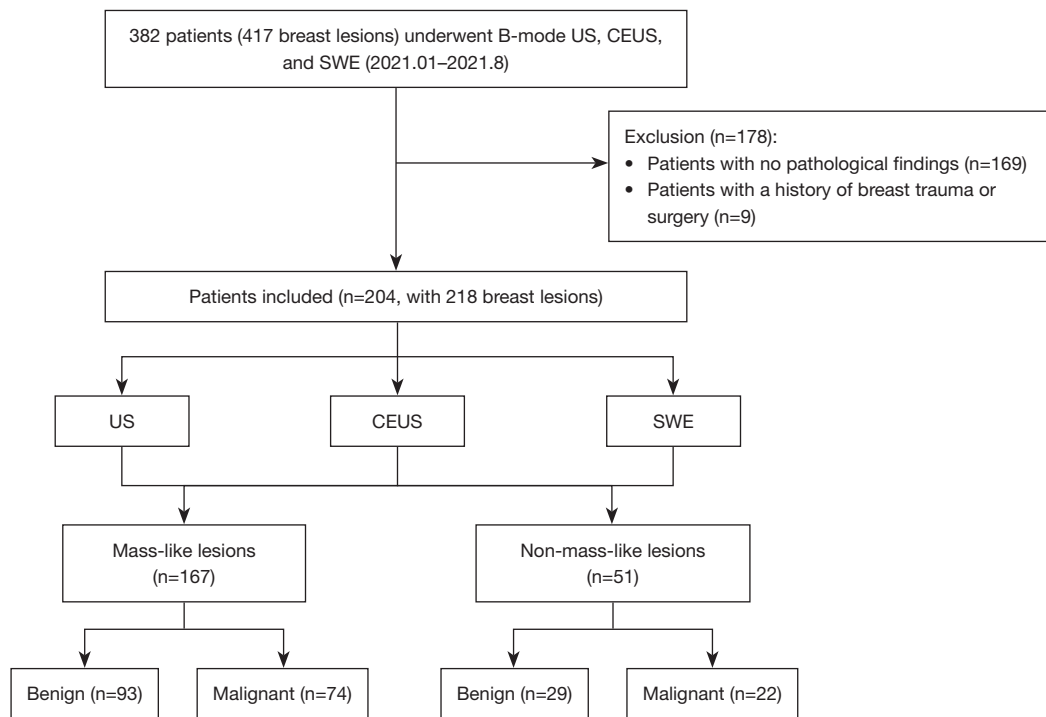


**Figure 1** Research process flow chart. US, ultrasound; CEUS, contrast-enhanced ultrasound; SWE, shear wave elastography.

diagnostic efficacy of US combined with CEUS and SWE for NML and ML breast lesions has not been systematically studied or compared.

Therefore, the present study aimed to analyze the characteristic appearances of NML and ML lesions on conventional US, CEUS, and SWE and evaluate whether the diagnostic performances of these three ultrasonic techniques in differentiating benign from malignant breast lesions were different. We present the following article in accordance with the STARD reporting checklist (available at <https://gs.amegroups.com/article/view/10.21037/gs-23-51/rc>).

## Methods

### Baseline clinical data

From January to August 2021, 382 patients (417 breast lesions) underwent conventional US for the first time, followed by CEUS and SWE. Of these, a total of 204 female patients (mean age 45 years, range 22–74 years) with 218 breast lesions (mean diameter 2.12 cm, range 0.4–10 cm) were included in this study, all of which had undergone surgical excision, ultrasound-guided core needle aspiration

biopsy or aspiration biopsy after multimodal ultrasound.

**Inclusion criteria:** lesions diagnosed as breast lesions by conventional US, CEUS, and SWE, with clear pathological diagnosis results, clinical pathology, and follow-up data.

**Exclusion criteria:** a history of neoadjuvant chemotherapy or radiotherapy for breast diseases; allergies to eggs, milk, or seafood; and pregnancy or lactation.

*Figure 1* shows a flow chart of the research process. The ethics committee of the First Medical Center of PLA General Hospital approved this study (No. S2021-683-01). The included patients provided written informed consent to participate in the study, and the study was conducted according to the Declaration of Helsinki (as revised in 2013).

### Instruments and methods

#### US and CEUS

The Minray Resona 7s ultrasonic instrument (Mindray Medical International, Shenzhen, China) was adapted with an L11-3U (5.6–10 MHz) linear transducer for conventional US and an L11-3U linear array probe (4–9 MHz) for CEUS. Patients maintained supine or lateral positions to expose the bilateral breasts and axillary region. After a routine

examination of the breast and axillary region, the location, size, shape, and blood flow of the lesions were recorded. Following the selection of sections with the most abundant blood flow, the machine was adjusted to the imaging mode, and a 5 mL SonoVue contrast agent was intravenously injected. The physician began to record real-time dynamic images (up to 180 seconds) of breast lesions while the assistants injected the contrast agents. The images were saved for further investigation. After CEUS, the patient was observed for 30 minutes and those without adverse reactions could leave.

### SWE

The Aixplorer® ultrasonic diagnostic system (SuperSonic Imagine, Aix-en-Provence, France), with a transducer frequency of 4–12 MHz, was adopted for the SWE inspections. The probe was moved slowly and smoothly perpendicular to the skin, and the patients were asked to breathe after showing the nodules. After selecting the region of interest, the sampling box covered all lesions, especially in the hardest part. The clarity of the image was adjusted to obtain a stable and repeatable image. The maximum, average, and minimum elasticity of lesion tissues at three different sections were recorded, and the elasticity ratio of the lesion to the peripheral parenchyma at the same depth was measured. In addition, the existence of a “stiff rim sign” was also recorded.

### Image analysis

US, CEUS, and SWE images were collected and interpreted by two ultrasound physicians with more than 3 years of experience. According to the fifth edition of the BI-RADS Classification System, the lesions were subdivided into 3, 4a, 4b, 4c, and 5 categories. The location of breast lesions was recorded using the clock method. In addition, the size, shape, number, orientation, internal echo, edge, capsule, calcification, and attenuation of breast lesions were recorded. For NML lesions, we also recorded whether the lesion was related to the catheter and was accompanied by structural distortion and other characteristic ultrasonic manifestations. Adler classification was employed to record the color blood flow of the lesion. CEUS evaluated the enhancement mode, contrast agent distribution, enhancement intensity, enhancement direction, lesion range, enhancement sharpness, margin, perfusion defects, peripheral blood vessel, and regression time. The enhancement range >3 mm was used as the criterion for judging the extension of the enhancement area compared

with conventional ultrasound images.

### Statistical analysis

SPSS 23.0 (IBM Corporation, Armonk, NY) statistical software was used for statistical analysis. Continuous variables conforming to a normal distribution were expressed as the mean ± standard deviation. The constant variables of non-normal distribution were expressed as medians (P25, P75). Classification variables were expressed as a percentage. The  $\chi^2$  test and Fisher test verified the qualitative parameters. The Mann-Whitney U test verified the maximum, average, and minimum elastic modulus, as well as the ratio to the surrounding elastic modulus because they do not conform to the normal distribution. The receiver operating characteristic (ROC) curve was plotted, and compared the diagnostic performance of US, US + CEUS, US + SWE, US + CEUS + SWE models using the area under the curve (AUC). In addition, the ROC curve is used to find the point closest to the upper left corner of the curve, namely the cut-off value. The cut-off value, sensitivity, and specificity of US, US + CEUS, US + SWE, US + CEUS + SWE were analyzed and compared. The Z-test was used to compare the differences between AUCs.  $P < 0.05$  was considered statistically significant.

## Results

### Pathological results

Pathologically, the 218 lesions included 96 malignant and 122 benign breast lesions. The included patients were assigned to the ML (1.8±1.4 cm) and the NML (3.3±1.9 cm) lesion groups. The ML lesions group included 93 benign lesions (1.4±0.7 cm) and 74 malignant lesions (2.3±1.8 cm), and the NML lesions group included 27 benign lesions (2.6±1.6 cm) and 20 malignant lesions (4.1±2.0 cm). The pathological information of the ML and NML groups is shown in detail in *Table 1*.

### Imaging features of the ML lesions group

*Table 2* lists the features of conventional US, CEUS, and SWE in the ML lesions. Patients over the age of 45 years had more malignant ML lesions than benign ML lesions ( $P < 0.05$ ). On conventional ultrasonography, posterior echo changes, unclear boundaries, irregular shape, and abundant blood supply were more common in malignant ML lesions

**Table 1** Clinical data of mass breast lesions and non-mass breast lesions

Pathological results	Mass-like lesions	Non-mass-like lesions	Total
Benign (n=122)			
Fibroadenoma	51	6	57
Mammary adenosis	19	12	31
Papilloma	11	7	18
Sclerosing adenosis	2	0	2
Phyllodes tumor	1	0	1
Cyst	7	0	7
Cyclomastopathy	1	3	4
Inflammation	1	0	1
Lipoma	0	1	1
Breast adenosis with pseudoangioma			
Malignant (n=96)			
Invasive ductal carcinoma	7	9	16
Intraductal carcinoma	0	1	1
Carcinoma <i>in situ</i>	1	0	1
Intraductal papillary carcinoma	1	0	1
Paget's disease	51	6	57
Lobular carcinoma <i>in situ</i>	19	12	31

than in benign ML lesions ( $P < 0.05$ ). On CEUS, malignant ML lesions mostly exhibited rapid progression, unevenness, and a high enhancement mode ( $P < 0.05$ ). Malignant ML lesions were often accompanied by an enlarged range and perforator vessels, unclear enhancement borders, irregular enhancement patterns, and a later regression time ( $P < 0.05$ ). On SWE, malignant ML lesions showed higher maximum, average, and minimum elastic modulus than benign ML lesions. In addition, the incidence of “stiff rim sign” in malignant ML lesions was significantly higher than that in benign ML lesions (*Figure 2*).

#### **Imaging features of the NML lesions group**

The characteristics of NML on conventional US, CEUS, and SWE are shown in *Table 3*. The incidence of calcification and an abundant blood flow signal in malignant NML lesions were higher than those in benign NML lesions ( $P < 0.05$ ). On CEUS, compared with benign NML, malignant NML

were more likely to exhibit the attributes of heterogeneous enhancement mode, increased lesion area and perforator vascular structure ( $P < 0.05$ ). On SWE, the mean, maximum, and minimum elastic modulus, and the ratio of the elastic modulus to surrounding tissue of malignant NML lesions were higher than those of benign NML lesions. In addition, malignant NML lesions had a higher probability of a “stiff rim sign” than benign NML lesions ( $P < 0.05$ ) (*Figure 3*).

#### **Comparative analysis of the clinical and imaging features of malignant ML and NML lesions**

The age, lesion size, ductal carcinoma in situ (DCIS), orientation, and “stiff rim sign” of malignant ML and NML lesions were compared and analyzed. Except for age, there were differences in lesion size, DCIS, orientation, and “stiff rim sign” ( $P < 0.05$ ). Compared with mass-type breast cancer, non-mass-type breast cancer is larger, grows in parallel, and is more likely to be accompanied by DCIS. The incidence of “stiff rim sign” in mass breast cancer was higher than in non-mass breast cancer ( $P < 0.05$ ). In addition, the human epidermal growth factor receptor 2 (HER2), estrogen receptor (ER), progesterone receptor (PR), and Ki-67 expression of malignant ML and NML lesions tested by immunohistochemistry were compared in this study, and the results showed that the expression of Ki-67 was higher in malignant ML lesions than that in malignant NML lesions ( $P < 0.05$ ) (*Table 4*).

#### **Comparison of the diagnostic performance of multimodal ultrasound**

The ROC curves of the various ultrasound detection modes for the different breast lesion groups are shown in *Figure 4*. In the ML group, the AUC of US + SWE + CEUS (0.976) was significantly higher than that of US (0.886), US + CEUS (0.936), and US + SWE (0.966) ( $P < 0.05$ ), indicating that US + CEUS + SWE has the best diagnostic efficiency for the ML group. For the NML group, US + SWE (0.935) had the highest AUC but showed no statistical difference with US + CEUS + SWE (0.874), indicating that both have high diagnostic power. For all breast lesions, the diagnostic efficacy of US + SWE (0.960) was the highest, and there was no significant difference between US + CEUS + SWE (0.958) and US + SWE ( $P > 0.05$ ), indicating that both US + CEUS + SWE and US + SWE had higher diagnostic efficacy for breast lesions.

*Table 5* shows the sensitivity, specificity, and AUC of

**Table 2** US, CEUS and SWE imaging features of the ML lesions group

Features	Benign	Malignant	$\chi^2/t$	P
Age (years)			12.223	0.000
<45	58 (62.4%)	26 (35.1%)		
≥45	35 (37.6%)	48 (64.9%)		
Calcifications			0.394	0.530
Absent	67 (72.0%)	50 (67.6%)		
Present	26 (28.0%)	24 (32.4%)		
Orientation			1.579	0.209
Parallel	64 (68.8%)	44 (59.5%)		
Non-parallel	29 (31.2%)	30 (40.5%)		
Color Doppler			39.167	0.000
Grade 0	37 (39.8%)	7 (9.5%)		
Grade 1	32 (34.4%)	26 (35.1%)		
Grade 2	9 (9.7%)	22 (29.7%)		
Grade 3	3 (3.2%)	16 (21.6%)		
Peripheral blood flow	12 (12.9%)	3 (4.1%)		
Lesion sharpness			18.129	0.000
Round	20 (21.5%)	2 (2.7%)		
Oval	19 (20.4%)	8 (10.8%)		
Irregular	54 (58.1%)	64 (86.5%)		
Lesion margin			39.357	0.000
Clear	30 (32.3%)	3 (4.1%)		
Unclear	32 (34.4%)	16 (21.6%)		
Spiculated	23 (24.7%)	24 (32.4%)		
Angular	8 (8.6%)	31 (41.9%)		
Posterior echo			6.277	0.043
Attenuation	24 (25.8%)	17 (23.3%)		
Enhancement	6 (6.5%)	14 (19.2%)		
No change	63 (67.7%)	42 (57.5%)		
CEUS				
Wash-in time			23.548	0.000
Early	52 (55.9%)	66 (89.2%)		
Synchronous	23 (24.7%)	7 (9.5%)		
Later	18 (19.4%)	1 (1.4%)		
Enhanced intensity			42.562	0.000
Hyper-enhanced	44 (47.3%)	70 (94.6%)		
Iso-enhanced	29 (31.2%)	2 (2.7%)		
Hypo-enhanced	20 (21.5%)	2 (2.7%)		

Table 2 (continued)

Table 2 (continued)

Features	Benign	Malignant	$\chi^2/t$	P
Enhancement direction			13.256	0.001
Centripetal	12 (12.9%)	21 (28.4%)		
Centrifugal	20 (21.5%)	25 (33.8%)		
Diffuse	61 (65.6%)	28 (37.8%)		
Enhancement mode			7.911	0.005
Homogeneous	17 (18.3%)	3 (4.1%)		
Heterogeneous	76 (81.7%)	71 (95.9%)		
Lesion range			78.205	0.000
Without increase	84 (90.3%)	17 (23.0%)		
Increase	9 (9.7%)	57 (77.0%)		
Peripheral blood vessel			58.608	0.000
No	73 (78.5%)	14 (18.9%)		
Yes	20 (21.5%)	60 (81.1%)		
Enhancement sharpness			25.069	0.000
Regular	38 (40.9%)	5 (6.8%)		
Irregular	55 (59.1%)	69 (93.2%)		
Enhancement margin			25.069	0.000
Clear	38 (40.9%)	5 (6.8%)		
Unclear	55 (59.1%)	69 (93.2%)		
Wash-out time			33.055	0.000
Early	3 (3.2%)	3 (4.1%)		
Synchronous	38 (40.9%)	2 (2.7%)		
Later	52 (55.9%)	69 (93.2%)		
SWE				
Mean*	23.900 (16.317, 37.102)	76.795 (54.348, 110.393)	832.000	0.000
Max*	35.950 (21.887, 49.790)	104.720 (75.573, 143.230)	778.500	0.000
Min*	15.370 (11.015, 29.667)	45.250 (22.875, 71.827)	1537.000	0.000
Ratio*	1.600 (1.147, 2.445)	5.115 (3.568, 7.581)	914.500	0.000
Stiff rim			110.040	0.000
Yes	12 (12.9%)	70 (94.6%)		
No	81 (87.1%)	4 (5.4%)		

\* , constant variables that are not normally distributed are expressed by median (P25, P75). US, ultrasound; CEUS, contrast-enhanced ultrasound; SWE, shear wave elastography; ML, mass-like.

these several ultrasound techniques. US + SWE had the highest sensitivity and specificity in diagnosing all breast lesions. For the ML and NML groups, US + SWE + CEUS had the highest sensitivity and specificity. As for the ML

group, US + CEUS + SWE had the highest sensitivity (95.9%), specificity (90.3%), and AUC (0.976), which were higher than those of the total breast group (92.7%, 90.2%, and 0.958, respectively) and NML group (91.3%, 79.3%,

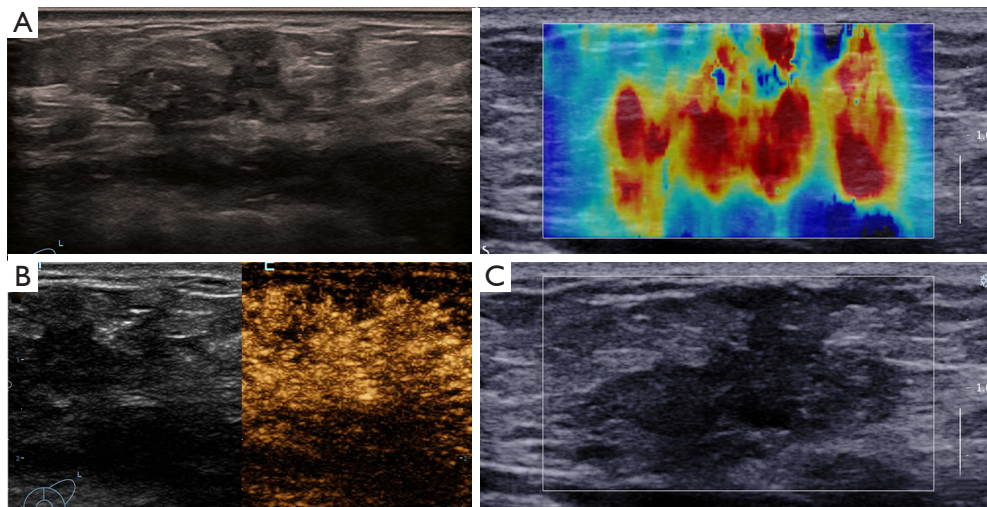


**Figure 2** Multimodal ultrasound images of a 35-year-old woman with invasive breast cancer. (A) On US, the lesion appeared as an irregularly shaped patchy area of low echo. (B) On CEUS, the lesions showed rapid and high enhancement, and the range was significantly increased. (C) On SWE, the average elastic modulus was 113.5 kPa, the maximum elastic modulus was 167.47 kPa, and the minimum elastic modulus was 83.6 kPa. The ratio of elastic modulus to surrounding tissue was 7.1. US, ultrasound; CEUS, contrast-enhanced ultrasound; SWE, shear wave elastography.

and 0.874, respectively).

## Discussion

US applies to the small and dense breasts of Chinese women (28). However, due to NML lesions showing no space-occupying effect on conventional US, some difficulties still exist in preoperative US diagnosis (29). Therefore, our research investigated whether multimodal ultrasound could improve the diagnostic efficiency of NML compared with ML lesions.

The pathological manifestations of NML and ML vary. Previous studies have shown that adenomas are the most common NML lesions, as compared to cystic fibrosis, fibroadenomas, sclerosing adenomas, inflammation, atypical ductal hyperplasia, and intraductal papillomas (7,8). In terms of malignant NML lesions, DCIS is more common than invasive ductal carcinoma and invasive lobular carcinoma (29,30). Our research results are consistent with the previously reported findings. With the incidence and development of breast lesions, many breast lesions may manifest as ML on ultrasound. Therefore, identifying optimum and malignant breast lesions in various periods for subsequent treatment is particularly important.

The incidence of ML lesions is high and is accompanied by obvious boundaries on conventional ultrasound, which

is more common than NML lesions (30). Among the malignant ML cases included in this study, those >45 years old, rich blood supply, irregular shape, angular or spiculated borders, and posterior echo changes were detected more frequently, which is consistent with previous research findings. Li *et al.* (31) showed that the ability of tumor cells (as reflected by morphological changes) increases and proliferates to a certain extent, highlighting the malignant transformation of cells.

In the CEUS mode, malignant ML lesions had a higher probability of fast entry and slow exit, high enhancement, uneven enhancement, enlarged range, accompanying perforator vascular structure, irregular boundary, and unclear boundary than benign ML lesions. Typical malignant lesions often have a rich blood flow, unstable blood vessels, varying diameters, and incomplete vascular walls, leading to the rapid perfusion of tumors. The enlargement of the enhancement area may reflect the true density and distribution of microvessels in malignant lesions (32). The incidence of high enhancement in malignant lesions (94.6%) is higher than that in benign lesions (47.3%), which may be due to the increase in the number of vessels in tumor tissues caused by the stimulation of tumor angiogenesis factors (32). Also, owing to the dense distribution of blood vessels and the lack of a thin new vascular wall in the muscular layer, the formed



**Table 3** US, CEUS, and SWE imaging features of the NML lesions group

Features	Benign	Malignant	$\chi^2/z$	P
Age (years)			3.814	0.051
<45	21 (72.4%)	10 (45.5%)		
≥45	8 (27.6%)	12 (54.5%)		
Calcifications			4.948	0.041
Absent	22 (75.9%)	10 (45.5%)		
Present	7 (24.1%)	12 (54.5%)		
Orientation				1.000
Parallel	27 (93.1%)	21 (95.5%)		
Non-parallel	2 (6.9%)	1 (4.5%)		
Color Doppler				0.011
Grade 0	9 (31.0%)	1 (4.5%)		
Grade 1	14 (48.3%)	8 (36.4%)		
Grade 2	3 (10.3%)	6 (27.3%)		
Grade 3	1 (3.4%)	6 (27.3%)		
Peripheral blood flow	2 (6.9%)	1 (4.5%)		
Posterior echo				0.173
Attenuation	4 (13.8%)	7 (31.8%)		
No change	25 (86.2%)	15 (68.2%)		
CEUS				
Wash-in time				0.170
Early	22 (75.9%)	21 (95.5%)		
Synchronous	5 (12.7%)	1 (4.5%)		
Later	2 (6.9%)	0 (0%)		
Enhanced intensity				0.840
Hyper-enhanced	24 (82.8%)	18 (81.8%)		
Iso-enhanced	4 (13.8%)	4 (18.2%)		
Hypo-enhanced	1 (3.4%)	0 (0%)		
Enhancement direction				0.185
Centripetal	6 (20.7%)	10 (49.5%)		
Centrifugal	2 (6.9%)	1 (4.5%)		
Diffuse	20 (72.6%)	11 (50.0%)		
Enhancement mode				0.015
Homogeneous	7 (24.1%)	0 (0%)		
Heterogeneous	22 (75.9%)	22 (100%)		

**Table 3** (continued)

Table 3 (continued)

Features	Benign	Malignant	$\chi^2/z$	P
Lesion range			20.812	0.000
Without increase	25 (86.2%)	5 (22.7%)		
Increase	4 (13.8%)	17 (77.3%)		
Peripheral blood vessel			9.233	0.002
No	16 (55.2%)	3 (13.6%)		
Yes	13 (44.8%)	19 (86.4%)		
Enhancement sharpness				0.062
Regular	5 (17.2%)	0 (0%)		
Irregular	24 (82.8%)	22 (100%)		
Enhancement margin				0.062
Clear	5 (17.2%)	0 (0%)		
Unclear	24 (82.8%)	22 (100%)		
Wash-out time				0.160
Early	1 (3.4%)	0 (0%)		
Synchronous	6 (20.7%)	1 (4.5%)		
Later	22 (75.9%)	21 (95.5%)		
SWE				
Mean*	18.60 (13.73, 33.30)	89.43 (39.50, 129.87)		0.000
Max*	22.00 (15.88, 66.08)	118.5 (56.44, 174.24)		0.000
Min*	12.37 (7.70, 32.06)	63.61 (19.93, 87.91)		0.000
Ratio*	1.47 (1.10, 2.88)	4.47 (3.02, 6.85)		0.000
Stiff rim			16.415	0.000
Yes	27 (93.1%)	9 (40.9%)		
No	2 (6.9%)	13 (59.1%)		

\*, constant variables that are not normally distributed are expressed by median (P25, P75). US, ultrasound; CEUS, contrast-enhanced ultrasound; SWE, shear wave elastography; NML, non-mass-like.

arteriovenous fistula may lead to a greater internal blood flow increase (14).

In the SWE mode, the probability of malignant ML lesions with high maximum, average, and minimum elastic modulus; elastic modulus ratio; and “stiff rim sign” was higher than that of benign ML, which was similar to previous studies (13,33). The increased hardness of breast cancer seems to be related to the nature of collagen produced by tumor-associated stromal cells [fibroblasts and cancer-associated fibroblasts (CAFs)] (34). With the increase of matrix stiffness, CAFs activate myofibroblasts to express

$\alpha$ -smooth muscle actin ( $\alpha$ -SMA) and Snail1, resulting in higher contraction ability and maintenance of extracellular matrix (ECM) protein secretion, thereby promoting tissue sclerosis (35).

Calcification and rich blood flow are more common in malignant than in benign NML lesions. For NML lesions, 45 years of age is not a clear demarcation line of the high incidence of malignant breast lesions. The probability of enlarged range and trophoblastic vessels in malignant NML lesions was significantly higher than that in benign NML lesions. Xu *et al.* (8) reported that malignant NML

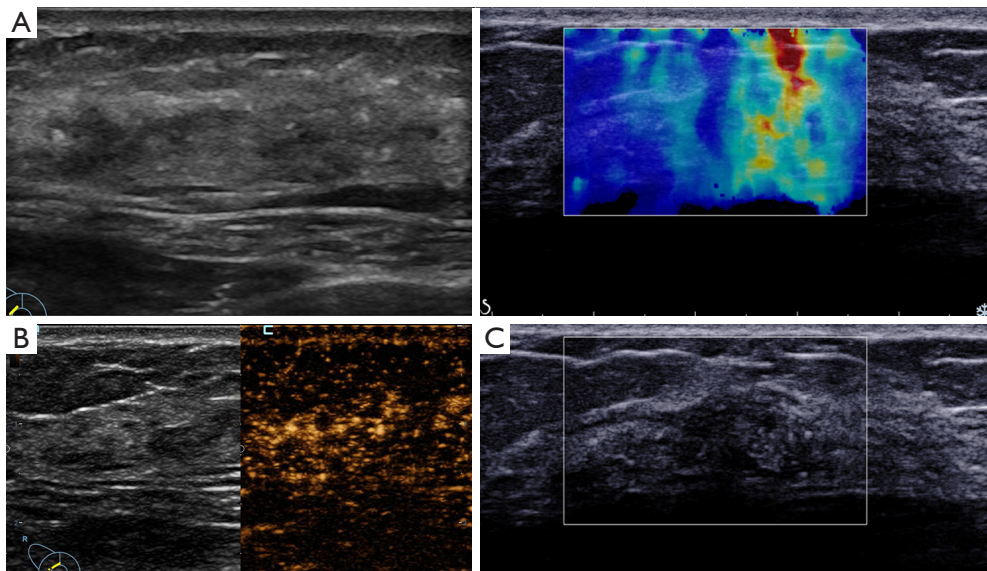


**Figure 3** Multimodal ultrasound images of a 36-year-old female presented with DCIS. (A) On US, the lesion appeared as an irregularly shaped patchy area of low echo. (B) On CEUS, the lesion showed synchronous equal enhancement, and the range did not increase significantly. (C) The average elastic modulus was 117.0 kPa, the maximum elastic modulus was 127.8 kPa, the minimum elastic modulus was 99.53 kPa, and the ratio of elastic modulus to surrounding tissue was 4.7. DCIS, ductal carcinoma in situ; US, ultrasound; CEUS, contrast-enhanced ultrasound.

lesions also showed the same characteristics in CEUS. In our view, like ML, the increased scope of NML lesions on CEUS and the appearance of peripheral blood vessels reflect the formation of abnormal blood vessels. On SWE, the maximum, average, and minimum elastic modulus of malignant NML lesions were higher than those of benign NML lesions, and the “stiff rim sign” is more likely to appear in malignant than benign NML lesions. Ko *et al.* (36) showed that SWE could improve the positive predictive value of BI-RADS 4a NML.

Compared with mass breast cancer, non-mass breast cancer was larger, exhibited parallel growth, and was more likely to be accompanied by DCIS ( $P < 0.05$ ), which is consistent with previous literature reports (37). Numerous studies have shown that many DCIS cases often manifest as NML lesions under conventional US (32,38). According to Jiang *et al.*, DCIS or micro-invasive DCIS is the main pathological type of NML (89.5%) (30), which is higher than that in our study (85.7%). The size of malignant NML lesions is significantly larger than that of malignant ML lesions, which may be attributable to its undetectability in patients that are late to the hospital. In addition, although 40.5% of malignant breast tumors in this study showed a longitudinal growth trend (7), 93.61%

(44/47) of the transverse diameters of NML lesions in this study were parallel to the breast. Moreover, the “stiff rim sign” detection rate in non-tumorous breast cancer was lower than that in tumorous breast cancer. This may be due to increased collagen fibers around breast cancer lesions, making the breast cancer appear as a mass. In the present study, the expression of Ki-67 in malignant NML was lower than that in malignant ML ( $P < 0.05$ ), suggesting that the proliferative activity of Ki-67-positive breast cancer was higher than that of the surrounding tissue, and the morphology could easily show a mass type. However, Sotome *et al.* (39) reported that Ki-67 showed no significant difference between the lump-type and malignant NML. Therefore, whether Ki-67-positive is related to the ultrasonic morphological characteristics of malignant ML and NML still needs to be further investigated.

A previous study showed that the sensitivity of conventional US for the diagnosis of NML lesions was only 75.0% but its specificity was only 76.5% (39). In our study, the sensitivity of conventional ultrasound to NML decreased (65.2%) but the specificity increased (89.7%) compared to that reported in previous studies. In the combined diagnostic effect of multiple ultrasound methods, the sensitivity of US + CEUS + SWE was higher (95.2%),

**Table 4** Clinical and imaging features of malignant ML and NML

Prognostic factors	Malignant NML	Malignant ML	P
Age (years)			0.707
≤45	9 (40.9%)	27 (36.5%)	
>45	13 (59.1%)	47 (63.5%)	
Lesion size			0.005
≤20	5 (22.7%)	43 (58.1%)	
21–50	11 (50.0%)	26 (35.1%)	
≥51	6 (27.3%)	5 (6.8%)	
With DCIS			0.001
Present	19 (86.4%)	41 (55.4%)	
Absent	3 (13.6%)	33 (44.6%)	
Orientation			0.002
Parallel	21 (95.5%)	44 (59.5%)	
Non-parallel	1 (4.5%)	30 (40.5%)	
Stiff rim			0.003
Yes	14 (63.6%)	68 (91.9%)	
No	8 (34.4%)	6 (8.1%)	
ER			0.634
–	26.3% (5/19)	21.1% (12/57)	
+	73.7% (14/19)	78.9% (45/57)	
PR			0.608
–	26.3% (2/19)	20.7% (12/58)	
+	73.7% (14/19)	79.3% (46/58)	
HER2			0.250
–	44.4% (4/9)	65.6% (21/32)	
+	55.6% (5/9)	34.3% (11/32)	
Ki-67			0.045
–	52.6% (10/19)	27.6% (16/58)	
+	47.4% (9/19)	72.4% (42/58)	

ML, mass-like; NML, non-mass-like; DCIS, ductal carcinoma in situ; ER, estrogen receptor; PR, progesterone receptor; HER2, human epidermal growth factor receptor 2.

while the specificity was lower (79.3%). Previous studies have shown that fibrocystic changes with calcification and sclerosing adenosis can become false-positive NML (30,40). The sensitivity and specificity of US + CEUS + SWE in the ML group were 95.9% and 90.3%, respectively. For

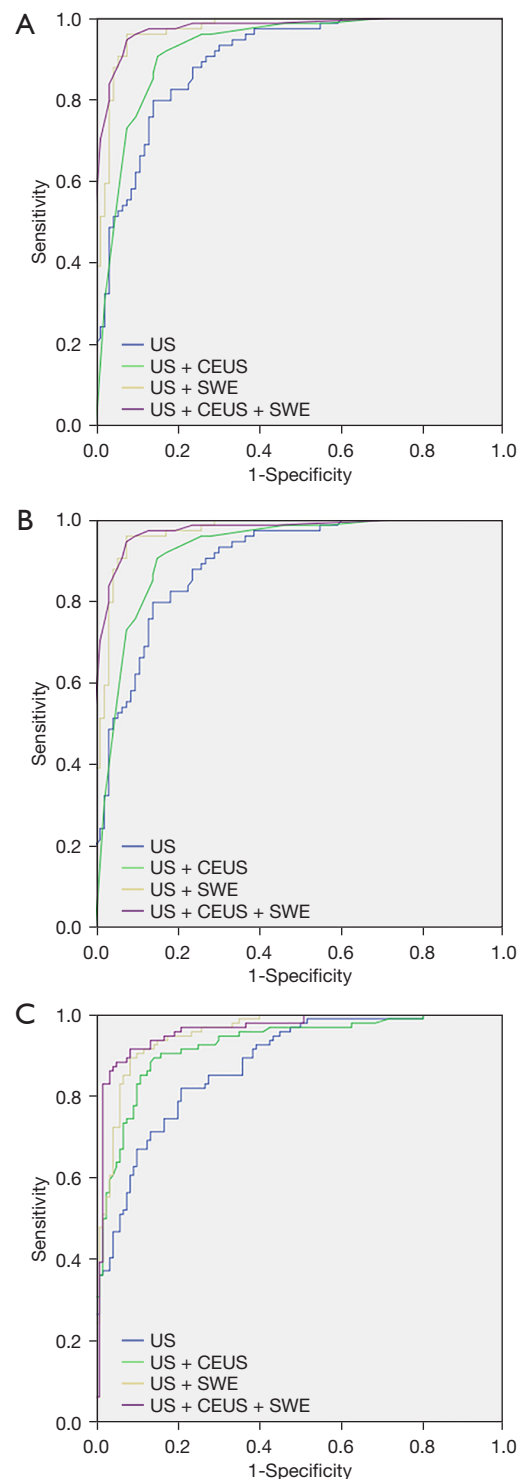


**Figure 4** Comparison of the diagnostic performance of US, US + CEUS, US + SWE, US + CEUS + SWE for ML lesions (A), NML lesions (B), and all breast lesions (C). US, ultrasound; CEUS, contrast-enhanced ultrasound; SWE, shear wave elastography; ML, mass-like; NML, non-mass-like.

**Table 5** Sensitivity, specificity, and AUC of US, US + CEUS, US + SWE, US + CEUS + SWE, and US + CEUS + SWE

Group	US			US + CEUS			US + SWE			US + CEUS + SWE					
	Sensitivity	Specificity	AUC	Sensitivity	Specificity	AUC	P	Sensitivity	Specificity	AUC	P	Sensitivity	Specificity	AUC	P
Total	78.7%	81.8%	0.861 (0.808–0.904)	83.2%	88.5%	0.917 (0.872–0.905)	0.0010	89.5%	92.6%	0.960 (0.924–0.982)	0.0001	92.7%	90.2%	0.958 (0.922–0.980)	0.0001
ML	74.0%	89.2%	0.886 (0.828–0.930)	94.6%	82.8%	0.938 (0.891–0.970)	0.0120	95.9%	92.5%	0.966 (0.926–0.988)	0.0008	95.9%	90.3%	0.976 (0.940–0.993)	0.0002
NML	65.2%	89.7%	0.786 (0.650–0.887)	78.3%	82.8%	0.805 (0.672–0.902)	0.7834	91.3%	89.7%	0.935 (0.829–0.985)	0.0149	91.3%	79.3%	0.874 (0.753–0.95)	0.2104

AUC, area under the curve; US, ultrasound; CEUS, contrast-enhanced ultrasound; SWE, shear wave elastography; ML, mass-like; NML, non-mass-like.

all breast lesions, US + CEUS + SWE and US + SWE showed high diagnostic values, and there was no statistical significance in the AUC between them ( $P > 0.05$ ). Also, consistent with the results of Liu *et al.* (9), the sensitivity and specificity of US + CEUS + SWE were 97.7% and 93.2%, respectively. Furthermore, the sensitivity and specificity of US + CEUS + SWE in the ML group were the highest (95.9% and 90.3%, respectively), as was the area under the ROC curve (0.976), which was higher than that in the all breast lesions (92.7%, 90.2%, and 0.958, respectively) and NML (91.3%, 79.3%, and 0.874, respectively) groups. The results suggested that the diagnostic efficiency of US + CEUS + SWE for ML lesions is higher than that for NML lesions, which may be related to the ultrasonic morphology of breast lesions. ML lesions are more easily detected, observed, and diagnosed on ultrasound than NML lesions.

Our research still has some limitations. Firstly, the sample size of NML lesions was lower than that of ML lesions. Secondly, we did not assess the impact of different observers in the image feature analysis. Thirdly, a quantitative analysis of CEUS was not included in the study. Lastly, no further detailed classification of the ML and NML lesions was conducted.

## Conclusions

In conclusion, multimodal ultrasound can significantly improve the diagnostic efficiency of differentiating benign and malignant ML and NML lesions. Multimodal ultrasound showed higher diagnostic efficiency for ML lesions than for NML lesions.

## Acknowledgments

**Funding:** This work was supported by the National Natural Science Foundation of China (No. 82071925), the Military Health Special Research Project (No. 22BJZ23), the National Key Research and Development Program of China (No. 2019YFC0118800), and the Equipment Comprehensive Research Project (No. LB20211A010011).

## Footnote

**Reporting Checklist:** The authors have completed the STARD reporting checklist. Available at <https://gs.amegroups.com/article/view/10.21037/gS-23-51/rc>

**Data Sharing Statement:** Available at <https://gs.amegroups.com>

[com/article/view/10.21037/gs-23-51/dss](https://doi.org/10.21037/gland-surgery-2023-51)

Peer Review File: Available at <https://gs.amegroups.com/article/view/10.21037/gs-23-51/prf>

*Conflicts of Interest:* All authors have completed the ICMJE uniform disclosure form (available at <https://gs.amegroups.com/article/view/10.21037/gs-23-51/coif>). The authors have no conflicts of interest to declare.

*Ethical Statement:* The authors are accountable for all aspects of the work in ensuring that questions related to the accuracy or integrity of any part of the work are appropriately investigated and resolved. The ethics committee of the First Medical Center of PLA General Hospital approved this study (No. S2021-683-01). The included patients provided written informed consent to participate in the study, and the study was conducted according to the Declaration of Helsinki (as revised in 2013).

*Open Access Statement:* This is an Open Access article distributed in accordance with the Creative Commons Attribution-NonCommercial-NoDerivs 4.0 International License (CC BY-NC-ND 4.0), which permits the non-commercial replication and distribution of the article with the strict proviso that no changes or edits are made and the original work is properly cited (including links to both the formal publication through the relevant DOI and the license). See: <https://creativecommons.org/licenses/by-nc-nd/4.0/>.

## References

1. Barzaman K, Karami J, Zarei Z, et al. Breast cancer: Biology, biomarkers, and treatments. *Int Immunopharmacol* 2020;84:106535.
2. Debieu V, De Caluwé A, Wang X, et al. Immunotherapy in breast cancer: an overview of current strategies and perspectives. *NPJ Breast Cancer* 2023;9:7.
3. Miller EA, Pinsky PF, Heckman-Stoddard BM, et al. Breast cancer risk prediction models and subsequent tumor characteristics. *Breast Cancer* 2020;27:662-9.
4. Kim BK, Ryu JM, Oh SJ, et al. Comparison of clinicopathological characteristics and prognosis in breast cancer patients with different Breast Imaging Reporting and Data System categories. *Ann Surg Treat Res* 2021;101:131-9.
5. Park KW, Park S, Shon I, et al. Non-mass lesions detected by breast US: stratification of cancer risk for clinical management. *Eur Radiol* 2021;31:1693-706.
6. Zhao Zhijin, Hou Size, Li Shuang et al. Application of Deep Learning to Reduce the Rate of Malignancy Among BI-RADS 4A Breast Lesions Based on Ultrasonography. *Ultrasound Med Biol*, 2022, 48: 2267-2275.
7. Zhang F, Jin L, Li G, et al. The role of contrast-enhanced ultrasound in the diagnosis of malignant non-mass breast lesions and exploration of diagnostic criteria. *Br J Radiol* 2021;94:20200880.
8. Xu P, Yang M, Liu Y, et al. Breast non-mass-like lesions on contrast-enhanced ultrasonography: Feature analysis, breast image reporting and data system classification assessment. *World J Clin Cases* 2020;8:700-12.
9. Liu G, Zhang MK, He Y, et al. BI-RADS 4 breast lesions: could multi-mode ultrasound be helpful for their diagnosis? *Gland Surg* 2019;8:258-70.
10. Zhou SC, Le J, Zhou J, et al. The Role of Contrast-Enhanced Ultrasound in the Diagnosis and Pathologic Response Prediction in Breast Cancer: A Meta-analysis and Systematic Review. *Clin Breast Cancer* 2020;20:e490-509.
11. Liu H, Wan J, Xu G, et al. Conventional US and 2-D Shear Wave Elastography of Virtual Touch Tissue Imaging Quantification: Correlation with Immunohistochemical Subtypes of Breast Cancer. *Ultrasound Med Biol* 2019;45:2612-22.
12. Li XL, Lu F, Zhu AQ, et al. Multimodal Ultrasound Imaging in Breast Imaging-Reporting and Data System 4 Breast Lesions: A Prediction Model for Malignancy. *Ultrasound Med Biol* 2020;46:3188-99.
13. Jiang H, Yu X, Zhang L, et al. Diagnostic values of shear wave elastography and strain elastography for breast lesions. *Rev Med Chil* 2020;148:1239-45.
14. Zhou P, Jin C, Lu J, et al. Modified Model for Diagnosing Breast Imaging Reporting and Data System Category 3 to 5 Breast Lesions: Retrospective Analysis and Nomogram Development. *J Ultrasound Med* 2021;40:151-61.
15. Li C, Yao M, Shao S, et al. Diagnostic efficacy of contrast-enhanced ultrasound for breast lesions of different sizes: a comparative study with magnetic resonance imaging. *Br J Radiol* 2020;93:20190932.
16. Tang L, Chen Y, Du Z, et al. A multicenter study of a contrast-enhanced ultrasound diagnostic classification of breast lesions. *Cancer Manag Res* 2019;11:2163-70.
17. Wang W, Zheng Y, Wu XF, et al. Value of contrast-enhanced ultrasound area ratio in identifying benign and malignant small breast masses. *Gland Surg* 2020;9:1486-94.
18. Shima H, Okuno T, Nakamura T, et al. Comparing the

- extent of breast cancer tumors through contrast-enhanced ultrasound vs B-mode, opposed with pathology: evergreen study. *Breast Cancer* 2021;28:405-13.
19. Vraika I, Panourgias E, Sifakis E, et al. Correlation Between Contrast-enhanced Ultrasound Characteristics (Qualitative and Quantitative) and Pathological Prognostic Factors in Breast Cancer. *In Vivo* 2018;32:945-54.
  20. Boca Bene I, Dudea SM, Ciurea AI. Contrast-Enhanced Ultrasonography in the Diagnosis and Treatment Modulation of Breast Cancer. *J Pers Med* 2021;11:81.
  21. Makal GB, Güvenç İ. The Role of Shear Wave Elastography in Differentiating Idiopathic Granulomatous Mastitis From Breast Cancer. *Acad Radiol* 2021;28:339-44.
  22. Zhang X, Liang M, Yang Z, et al. Deep Learning-Based Radiomics of B-Mode Ultrasonography and Shear-Wave Elastography: Improved Performance in Breast Mass Classification. *Front Oncol* 2020;10:1621.
  23. Liu G, Zhang MK, He Y, et al. Shear wave elasticity of breast lesions: would it be correlated with the extracellular matrix components? *Gland Surg* 2019;8:399-406.
  24. Athanasiou A, Tardivon A, Tanter M, et al. Breast lesions: quantitative elastography with supersonic shear imaging--preliminary results. *Radiology* 2010;256:297-303.
  25. Wang ZL, Li Y, Wan WB, et al. Shear-Wave Elastography: Could it be Helpful for the Diagnosis of Non-Mass-Like Breast Lesions? *Ultrasound Med Biol* 2017;43:83-90.
  26. Farooq F, Mubarak S, Shaikat S, et al. Value of Elastography in Differentiating Benign from Malignant Breast Lesions Keeping Histopathology as Gold Standard. *Cureus* 2019;11:e5861.
  27. He H, Wu X, Jiang M, et al. Diagnostic accuracy of contrast-enhanced ultrasound synchronized with shear wave elastography in the differential diagnosis of benign and malignant breast lesions: a diagnostic test. *Gland Surg* 2023;12:54-66.
  28. Shen S, Zhou Y, Xu Y, et al. A multi-centre randomised trial comparing ultrasound vs mammography for screening breast cancer in high-risk Chinese women. *Br J Cancer* 2015;112:998-1004.
  29. Zhang W, Xiao X, Xu X, et al. Non-Mass Breast Lesions on Ultrasound: Feature Exploration and Multimode Ultrasonic Diagnosis. *Ultrasound Med Biol* 2018;44:1703-11.
  30. Jiang L, Zhou Y, Wang Z, et al. Is there different correlation with prognostic factors between "non-mass" and "mass" type invasive ductal breast cancers? *Eur J Radiol* 2013;82:1404-9.
  31. Li L, Zhou X, Zhao X, et al. B-Mode Ultrasound Combined with Color Doppler and Strain Elastography in the Diagnosis of Non-mass Breast Lesions: A Prospective Study. *Ultrasound Med Biol* 2017;43:2582-90.
  32. Li W, Zhou Q, Xia S, et al. Application of Contrast-Enhanced Ultrasound in the Diagnosis of Ductal Carcinoma In Situ: Analysis of 127 Cases. *J Ultrasound Med* 2020;39:39-50.
  33. Yoo J, Seo BK, Park EK, et al. Tumor stiffness measured by shear wave elastography correlates with tumor hypoxia as well as histologic biomarkers in breast cancer. *Cancer Imaging* 2020;20:85.
  34. Wang ZL, Sun L, Li Y, et al. Relationship between elasticity and collagen fiber content in breast disease: a preliminary report. *Ultrasonics* 2015;57:44-9.
  35. Evans A, Sim YT, Pourreyron C, et al. Pre-operative stromal stiffness measured by shear wave elastography is independently associated with breast cancer-specific survival. *Breast Cancer Res Treat* 2018;171:383-9.
  36. Ko KH, Jung HK, Kim SJ, et al. Potential role of shear-wave ultrasound elastography for the differential diagnosis of breast non-mass lesions: preliminary report. *Eur Radiol* 2014;24:305-11.
  37. Liu W, Zong M, Gong HY, et al. Comparison of Diagnostic Efficacy Between Contrast-Enhanced Ultrasound and DCE-MRI for Mass- and Non-Mass-Like Enhancement Types in Breast Lesions. *Cancer Manag Res* 2020;12:13567-78.
  38. Wang LC, Sullivan M, Du H, et al. US appearance of ductal carcinoma in situ. *Radiographics* 2013;33:213-28.
  39. Sotome K, Yamamoto Y, Hirano A, et al. The role of contrast enhanced MRI in the diagnosis of non-mass image-forming lesions on breast ultrasonography. *Breast Cancer* 2007;14:371-80.
  40. Wang ZL, Li N, Li M, et al. Non-mass-like lesions on breast ultrasound: classification and correlation with histology. *Radiol Med* 2015;120:905-10.
- (English Language Editor: A. Kassem)

**Cite this article as:** Li SY, Niu RL, Wang B, Jiang Y, Li JN, Liu G, Wang ZL. Determining whether the diagnostic value of B-ultrasound combined with contrast-enhanced ultrasound and shear wave elastography in breast mass-like and non-mass-like lesions differs: a diagnostic test. *Gland Surg* 2023;12(2):282-296. doi: 10.21037/gs-23-51